Mean-field theory for inhomogeneous electrolytes

Shin-Shing Yeh and Peilong Chen
Department of Physics and Center for Complex Systems, National Central University, Chungli 320, Taiwan
(Received 7 April 2005; published 19 September 2005)

We calculate the free energy density for inhomogeneous electrolytes based on the mean-field Debye-Hückel theory. Derived are the contributions of (1) the differential term for the electrolyte density being slow varying in one direction and (2) the boundary term for an electrolyte confined to one side of a planar interface. These contributions are shown to cause an electrolyte depletion near the air-water interfaces, which makes the surface tension increase, to be significantly larger than those predicted by previous theories. Nonuniform electrolyte densities are also computed near the water-electrolyte and electrolyte-electrolyte interfaces. Finally we calculate the interaction of two uncharged macrospheres due to the electrolyte depletion.

DOI: 10.1103/PhysRevE.72.036119 PACS number(s): 05.70.Np, 61.20.Qg, 68.35.Md

I. INTRODUCTION

The thermodynamics of charged particle fluids (electrolytes) is a long-standing problem. Eighty years ago a mean-field theory of electrolytes was published by Debye and Hückel [1]. The complicated interionic interactions are replaced by the mean potential obtained by solving the linearized Poisson-Boltzmann (PB) equation in the Debye-Hückel (DH) theory. In homogeneous systems the theory provides good predictions for dilute solutions [2]. In the next year, Wagner applied the theory to explain the increase of surface tension of an air-water interface when salts are added in the water [3]. In 1926 Bjerrum extended the theory to larger densities by associating positive and negative ions to form neutral dipole pairs [4]. Subsequently other formulations—for example, the integral equations [5]—are proposed to go beyond the mean-field level. Computational methods such as the Monte Carlo (MC) simulations [6] of charged particle systems were also actively studied in the last several decades.

The DH theory is also extended to other Coulomb systems. For example, the Debye-Hückel hole theory [7] extends the DH theory to one-component plasma by including an effective spherical cavity around an ion, inside which no other ions can penetrate. The generalized Debye-Hückel theory [8] obtained density correlations in the one-component plasma by functional differentiation of the DH theory generalized to nonuniform densities.

Integral equation formulations [5] are proposed to compute the correlation and fluctuation corrections neglected in the mean-field theory. However, in these theories the free energy cannot be defined explicitly, so it is hard to specify each source of correlations. On the other hand, density functional theories [9] treat correlation corrections by expressing the free energy as a functional of density distribution. The equilibrium in principle can be obtained by a variational method. However, the explicit form of the free energy density is largely unknown and approximations need to be made [10]. For example, inspired by the DH approach to the one-component plasma, one contribution from counterion correlations to the local density functional is proposed [11].

In this paper we propose that for nonuniform electrolyte distributions the local free energy density can be obtained in the mean-field level. We consider explicitly the simple case when the electrolyte density varies in one spatial direction, which commonly arises near a planar interface. In electrolytes with an air-water interface, Wagner [3] as well as Onsager and Samaras [12] added an image force to the mean force, obtained from the uniform distribution, to get a nonuniform distribution. In Sec. II, besides the image force, we show how a slow-varying nonuniform density leads to a modified linear PB equation based on the DH theory and contributes a differential correction term to the free energy density. We also derive another term contributed from the presence of an interface. The nonuniform and interface contributions are found to be more significant than the image force and give a depletion zone of ions near the interface significantly larger than previous theories. Considering finite ionic size leads to consistent values of the surface tension with experimental values at low concentrations.

In Sec. III we apply the formulation to two situations where electrolyte depletion is expected even when there is no dielectric discontinuity. In the first part the equilibrium density profile is calculated numerically when salts are confined to one side of an interface in water. The combined effects of the boundary and differential terms yield a depletion of ions from the interface, within the range of the Debye length. The interfacial density could be significantly lower than the bulk value, especially for ions with higher valences. In the second part the density profiles of two electrolytes separated by an interface are calculated for the application on the problem of ions transfer. The ratio of the interfacial to bulk density differences is found to decrease as the average bulk density is increased. At the end of Sec. III we apply the result to estimate the attraction induced by nonuniform electrolyte densities around two uncharged macrospheres. The effective depletion zone of ions contributes a weak attraction with larger ranges at lower electrolyte concentrations. At high concentrations the interaction is not expected to be significant because other energy scales, such as the van der Waal and dispersion forces, become important at short ranges.

II. SURFACE TENSION OF AN AIR-ELECTROLYTE INTERFACE

A. Introduction

An aqueous solution of inorganic salts was known to have a higher surface tension than pure water [13]. Wagner sug-

gested that the salt depletion near the surface is mainly caused by the electrostatic repulsion between the ions and polarized interface, making the surface tension increase [3]. To calculate such effects, consider a semi-infinite electrolyte with an air-water interface located at $z=0$. The density profile n_s of the s-type ions at a distance z from the interface is directly given by the Boltzmann formula

$$n_s(z) = n_s e^{-\beta W_s(z)}, \tag{1}$$

where $\beta=1/k_BT$, k_B the Boltzmann constant, T the temperature, and $W_s(z)$ the potential of mean force. For an 1:1 electrolyte, $W_+=W_-\equiv W$ and $n_+=n_-\equiv n$. $W(z_0)$ can be calculated as the work to bring an ion from infinity to z_0. The repulsive force felt by this ion, due to the dielectric discontinuity produced by the interface, was replaced by the interaction between the ion and its image q' at $-z_0$. For an aqueous solution at room temperature the dielectric constant ratio between water and air is about 80:1; thus, Wagner proposed that $q'=(\epsilon-\epsilon')q/(\epsilon+\epsilon')\approx q$. In an electrolyte, the electrostatic potential Φ, with the presence of the fixed ion, satisfies the equation

$$\nabla^2\Phi(\boldsymbol{r},z_0) - \kappa^2\Phi(\boldsymbol{r},z_0) = -\frac{q}{\epsilon}\delta(\boldsymbol{r},z_0), \tag{2}$$

with $\kappa^2(z_0)\equiv 2\beta n(z_0)q^2/\epsilon$. Here the potential of mean force was approximated by the mean electrostatic potential ($q\Phi$) and the second term on the left is obtained by the linearization (assuming low electrolyte densities) of the Boltzmann factor [2]. Onsager and Samaras (OS) replaced $\kappa(z_0)$ with the bulk value $\kappa(\infty)$ to simplify the calculation [12]. The electrostatic potential then becomes

$$\Phi = \frac{q}{4\pi\epsilon}\left(\frac{e^{-\kappa|\boldsymbol{r}-z_0\hat{z}|}}{|\boldsymbol{r}-z_0\hat{z}|} + \frac{e^{-\kappa|\boldsymbol{r}+z_0\hat{z}|}}{|\boldsymbol{r}+z_0\hat{z}|}\right), \tag{3}$$

where the first term is the well-known solution of Eq. (2) and the second term is the contribution from the image charges. $W(z)$ is calculated by integrating the repulsive force felt by the ion from infinity to z [12] as

$$W(z) = \frac{q^2}{4\pi\epsilon}\frac{e^{-2\kappa z}}{4z}.$$

The number density profile was obtained by substituting this expression into Eq. (1) as

$$n(z) = n_0 \exp\left(\frac{l_B e^{-2\kappa z}}{4z}\right). \tag{4}$$

Here n_0 is the density away from the interface and $l_B=\beta q^2/4\pi\epsilon\simeq 0.7$ nm at 300 K is the Bjerrum length. The negative adsorption would increase the surface tension according to the Gibbs-Duhem equation [14]. The OS theory gives fairly good agreement with experiments for concentrations up to $0.1M$, but underestimates the surface tension at higher concentrations.

Recently Levin [15] calculated the free energy needed to create the interface to obtain the surface tension rather than using the Gibbs adsorption isotherm. From Eq. (3), the electrostatic potential φ felt by the ion, due to the other ions and the polarized interface, was first calculated as

$$\varphi = \lim_{\boldsymbol{r}\to z_0\hat{z}}\left[\Phi - \frac{q}{4\pi\epsilon|\boldsymbol{r}-z_0\hat{z}|}\right] = \frac{q}{4\pi\epsilon}\left(-\kappa + \frac{e^{-2\kappa z_0}}{2z_0}\right). \tag{5}$$

The electrostatic energy is thus

$$E = A\int_0^\infty qn(z_0)\varphi(z_0)dz_0,$$

where A is the cross section area on the x-y plane. Therefore, the electrostatic free energy density was computed by applying the Debye charging process, in which all the particles are simultaneously charged from zero to their full charge, as

$$F^{\mathrm{el}} = 2\int_0^1 E(\tau q)\frac{d\tau}{\tau}.$$

The surface energy is the difference of total free energies after adding the interface: $\sigma=\lim_{A\to\infty}(1/A)(F-F^{\mathrm{bulk}})$ where F includes F^{el} as well as the entropic contribution. For small concentrations the result, based on the linearized PB equation used by OS, reduced to the OS limiting law. By including the ionic size effect near the interface, the agreement between Levin's theory and experiments is good for higher salt concentrations.

However, it is obvious that these calculations, using the electrostatic potential in a homogeneous electrolyte to obtain the inhomogeneous density profile, are not self-consistent. Furthermore, the density inhomogeneity also contributes to the local free energy density. In the next subsection, we use a modified linear PB equation for an inhomogeneous electrolyte to compute the free energy density, then compare the resulting surface tension with previous theories and experiments.

B. Total free energy density

We start from the DH equation for an inhomogeneous electrolyte—i.e., Eq. (2) with κ a function of $\boldsymbol{r}$: $\kappa(\boldsymbol{r})$. If we denote Φ_0 as the solution of Eq. (2) with a constant κ, it is just the first term of Eq. (3). We write Φ to be the sum of Φ_0, with $\kappa=\kappa_0\equiv\kappa(z_0)$, and the inhomogeneous correction Φ_1. Substituting $\Phi=\Phi_0+\Phi_1$ into Eq. (2), we assume $n(z)$ to be slow varying and expand $n(z)$ at $n(z_0)$ with the Taylor series (note that $\kappa^2=2\beta nq^2/\epsilon$). Keeping only the terms up to n'' leads to (with the prime denoting the derivative in z)

$$\nabla^2\Phi_1 - \kappa_0^2\Phi_1 = \left[2\kappa_0\kappa_0'(z-z_0) + \frac{1}{2}\kappa_0^{2\prime\prime}(z-z_0)^2\right]\Phi_0$$

$$\equiv -\frac{q}{\epsilon}G\Phi_0,$$

where $\kappa_0'\equiv\kappa'(z_0)$ and $\kappa_0^{2\prime\prime}\equiv[\kappa^2(z)]''_{z_0}$. Since Φ_0 satisfies Eq. (2) with $\kappa=\kappa_0$, we know that Φ_0 is the Green's function for $\nabla^2-\kappa_0^2$ and Φ_1 can be obtained as

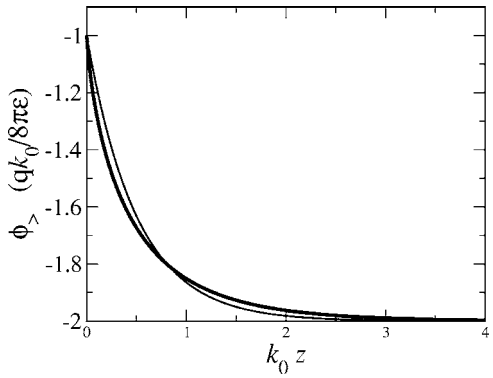

FIG. 1. Numerical results of Eq. (8) (thick line) and the approximating function of the first term of Eq. (10) (thin line).

$$\Phi_1(\boldsymbol{r},z_0)=\int \Phi_0(\boldsymbol{r},\boldsymbol{r}')G\Phi_0(\boldsymbol{r}',z_0)d\boldsymbol{r}'. \tag{6}$$

To calculate the electric potential φ felt by the fixed ion, we integrate over all charges, excluding the fixed ion. Since these charge distributions are $-\kappa^2\Phi$, from Eq. (2) we have

$$\begin{aligned}\varphi(\boldsymbol{r},z_0)&=\int \frac{-\epsilon\nabla^2\Phi(\boldsymbol{r}',z_0)-q\,\delta(\boldsymbol{r}'-z_0\hat{z})}{4\pi\epsilon|\boldsymbol{r}-\boldsymbol{r}'|}d\boldsymbol{r}'+\Phi_2\\&=\int \frac{-\kappa_0^2\Phi_0(\boldsymbol{r}',z_0)}{4\pi|\boldsymbol{r}-\boldsymbol{r}'|}d\boldsymbol{r}'+\Phi_1+\Phi_2.\end{aligned} \tag{7}$$

Here Φ_2 is the contribution from the images [as the second term in the last line of Eq. (5)]. In the second line we have substituted Φ with $\Phi_0+\Phi_1$ and use $\nabla^2\Phi_0-\kappa_0^2\Phi_0=(-q/\epsilon)\delta(\boldsymbol{r}-\boldsymbol{r}')$. We are interested in the potential $\varphi(z_0,z_0)$ felt by the ion fixed at $z_0\hat{z}$. Note that the system boundary affects the integration domain in Eq. (7). So for a semi-infinite electrolyte, where all ions are restricted to $z>0$, the first term in Eq. (7) becomes

$$\varphi_>(z_0,z_0)=\frac{-q\kappa_0^2}{16\pi^2\epsilon}\int_{z>0}\frac{e^{-\kappa_0|\boldsymbol{r}'-z_0\hat{z}|}}{|\boldsymbol{r}'-z_0\hat{z}|^2}d\boldsymbol{r}'. \tag{8}$$

Unfortunately we cannot calculate the integration analytically. Instead the numerical result is shown as the thick line in Fig. 1. To continue further in our analysis we approximate it with the function $(-q\kappa_0/4\pi\epsilon)(1-e^{-2\kappa_0 z_0}/2)$ which is drawn as the thin line in the figure.

The second term in Eq. (7) is obtained as [16]

$$\Phi_1(z_0,z_0)=\frac{q\kappa_0^{2\prime\prime}}{96\pi\epsilon\kappa_0^3}. \tag{9}$$

The potential felt by the test charge is thus

$$\varphi(z_0,z_0)\approx\frac{-q\kappa_0}{4\pi\epsilon}\left(1-\frac{e^{-2\kappa_0 z_0}}{2}\right)+\frac{q\kappa_0^{2\prime\prime}}{96\pi\epsilon\kappa_0^3}+\frac{q}{4\pi\epsilon}\frac{e^{-2\kappa_0 z_0}}{2z_0}, \tag{10}$$

where the last term is Φ_2, for which we use the result in Eq. (5). Now we are able to calculate F^{el} by using the Debye charging process:

$$F^{\mathrm{el}}=\frac{A}{12\pi\beta}\int_0^\infty\left(-\kappa_0^3[1-g(\kappa_0 z_0)-h(\kappa_0 z_0)]+\frac{\kappa_0^{2\prime\prime}}{8\kappa_0}\right)dz_0, \tag{11}$$

where $g(u)\equiv(3/8u^3)[1-e^{-2u}(1+2u+2u^2)]$ and $h(u)\equiv(3/8u^3)[1-e^{-2u}(1+2u)]$. Added with the entropic contribution of the ideal gas, the total free energy becomes

$$F=\frac{A}{12\pi\beta}\int_{-\infty}^\infty\left(-\kappa^3[1-g(\kappa z)-h(\kappa z)]+\frac{\kappa^{2\prime\prime}}{8\kappa}+3l_B^{-1}\kappa^2\ln\kappa^2\right)dz. \tag{12}$$

Here we have dropped the subscript of z_0 and $\kappa=\kappa(z)$. The term $-\kappa^3$ is the well-known electrostatic free energy density for a homogeneous electrolyte. We may note that $g(\kappa z)$ comes from the system boundary. At the boundary $z\to 0$, $[1-g(\kappa z)]\to\frac{1}{2}$, giving half of the bulk free energy density. At $z\to\infty$, $g(\kappa z)\to 0$, indicating a vanishing effect away from the interface. This extra term should yield a lower electrolyte density near the interface, due to the restricted amount of charges surrounding each ion. $h(\kappa z)$ is the image charge contribution. Near the interface $h(\kappa z\to 0)\to\infty$, reflecting the infinite repulsion given by the image charges. The second term $\kappa^{2\prime\prime}/8\kappa$ comes from the nonuniform electrolyte distribution, which is proportional to n''. There are no terms linear to n', since both n' and $-n'$ would give the same contribution. Considering this differential term, it is easy to show that a nonuniform density $n(z)=n_0+b\cos kz$ (with n_0, b, and k constants) always yields a higher F^{el} than $n(z)=n_0$. The differential term thus plays a role to retard local inhomogeneity.

The free energy in Eq. (12) is derived for an 1:1 electrolyte. It is straightforward to extend the derivation for the cases of multivalences. For an electrolyte in which positive ions have $+Z_+q$ charges and negative ions have $-Z_-q$ charges, the free energy is obtained as Eq. (12) with the parameter l_B replaced by $Z_+Z_-l_B$.

C. Density profile and surface tension

We compute numerically the density profile which minimizes the total free energy. For comparison first we use only the bulk, image charge, and entropic terms [Eq. (12) without the $g(\kappa z)$ and $\kappa^{2\prime\prime}/8\kappa$ terms]. The density profiles as shown in Fig. 2 (solid lines) are found to be consistent with those of OS (dot-dashed lines). As shown in the figure, the agreement between the solid and dot-dashed lines is fairly good, with $0.03M$ showing a better match than $0.99M$.

With the full F in Eq. (12), the density profiles are plotted in Fig. 2 as the dashed curves. The electrolyte densities near the interface are significantly less. At low concentrations, the depletion zone from full F is about 3 times larger than that for just considering the bulk, image, and entropic terms. One sees that the electrolyte inhomogeneity ($\kappa^{2\prime\prime}/8\kappa$ term) and boundary [$g(\kappa z)$ term] effects are significant for the depletion of the ions, besides the repulsion between the ions and polarized interface.

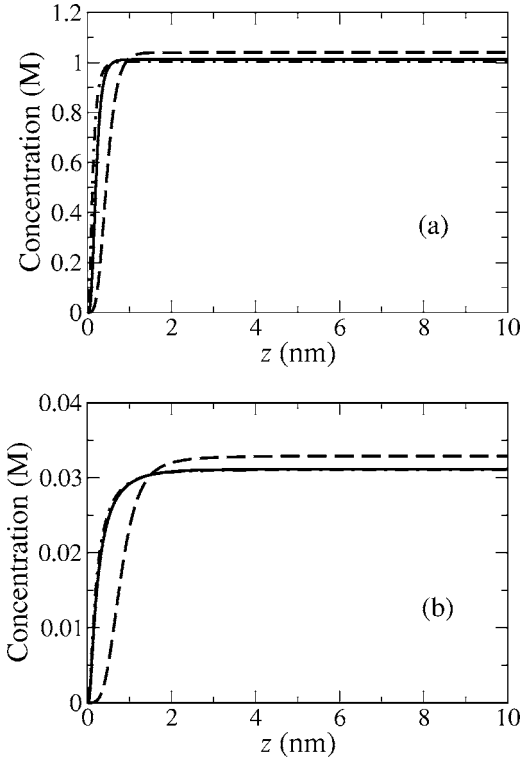

FIG. 2. The 1:1 electrolyte density profile versus distance from an air-electrolyte interface at (a) $0.03M$ and (b) $0.99M$. The dashed curve is obtained using Eq. (12). The solid curve shows the result using only the bulk, image, and entropic terms in Eq. (12). The dot-dashed curve is the result of the Onsager-Samaras theory.

Here we can check the approximation of keeping only the terms up to $n''(z)$. From the resulted density profile, the terms with higher-order derivatives are computed and their values are indeed negligible, indicating the validity of this approximation.

Similar results apply to the surface energy. The resulting surface tension from Eq. (12) is plotted in Fig. 3 as the solid line. It is almost twice larger than Levin's result (dotted line)

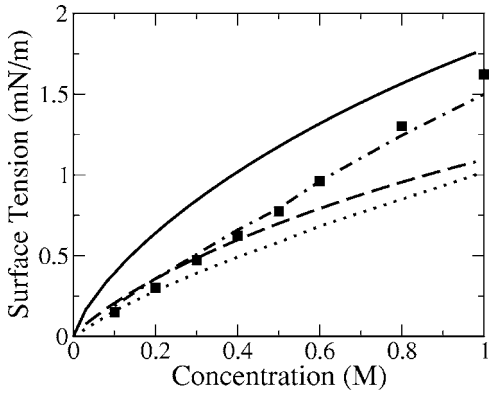

FIG. 3. The surface tension of an 1:1 electrolyte at room temperature versus the electrolyte concentration. The solid and dashed curves are the results of our calculations for $d=0$ and $d=0.21$ nm, respectively. Levin's predictions are shown as the dotted ($d=0$) and dot-dashed ($d=0.21$ nm) curves. The squares denote the experimental results [17] for NaCl.

at low electrolyte concentrations. This is expected from the larger amount of ions excluded near the interface due to the contributions from boundary and inhomogeneity as seen in Fig. 2.

However, to compare with experiments we also want to consider the effect of the finite ionic size d. The boundary condition for $n(z)$ would change with d. When $d=0$, $n(z=0)=0$ due to the infinite interaction between the ion and its image. With $d\neq 0$, $n(z)=0$ for $0<z<d$ but a finite value of n is allowed at $z=d$. With a finite value allowed at $z=d$, the size of depletion zone is found to decrease, leading to a smaller free energy difference and surface tension.

The calculation of NaCl ($d\approx 0.21$ nm) is shown in Fig. 3 as the dashed line. At low concentrations, the results (dashed line) match well to the experiment (squares) [17], but it is too low at high concentrations.

We believe that the comparisons at high electrolyte concentrations are not reliable. Several factors contribute to the error of prediction. All calculations are based on the DH theory, but it is well known that the DH theory fails in many situations with high electrolyte concentrations. For the surface tension, other factors are argued to dominate at high concentrations. (The correction due to the hydration radius of NaCl gives a remarkably good agreement with experiments in high concentrations in Levin's theory [15]; maybe we can only wait for more experimental data using different ions to know its validity.) For example, the dispersion force was proposed to be always larger than the image force for salt concentrations larger than $0.1M$ [18], suggesting that the electrostatic contribution cannot account for all the surface tension increases in experiments. The arguments also suggest that the dispersion forces may be important at low concentrations depending on ion specificity. Also the ionic size and hydration around the ions, which are short-range interactions, would play important roles to ionic distributions for concentrated electrolytes [19].

III. APPLICATION TO OTHER CASES

A. Depletion near a water-water interface

The presence of the boundary and inhomogeneity terms ($g(\kappa z)$ and $\kappa^{2''}/8\kappa$ term in the free energy density [Eq. (12)]) implies that the depletion of electrolytes still occurs even without dielectric discontinuity—e.g., a semi-infinite electrolyte with a water-water interface. We compute the total free energy density, dropping the contribution of the images [$h(\kappa z)$] from Eq. (12). The computed electrolyte density profile for an 1:1 electrolyte with an averaged density $C_0=0.03M$ is plotted as the solid line in Fig. 4. As expected the interfacial electrolyte density C_b is smaller than C_0 with a depletion zone on the scale of the Debye length. The result for a 2:2 electrolyte (dashed line) is also shown in Fig. 4 where F^{el} becomes more important than F^{entropic}. The interfacial density (dashed line in Fig. 4) is lower than that for the 1:1 electrolyte.

In Fig. 5 the ratios C_b/C_0 are shown for the 1:1, 1:2, and 2:2 electrolytes. The ratio decreases as the C_0 increases, indicating that the boundary effect is more important at high

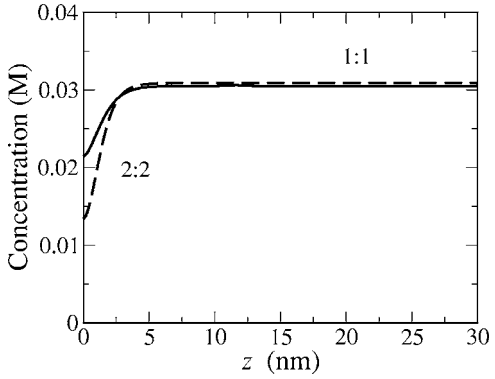

FIG. 4. The electrolyte density profiles with a water-electrolyte interface. For 1:1 and 2:2 electrolytes, the profiles are shown as the solid and dashed lines respectively.

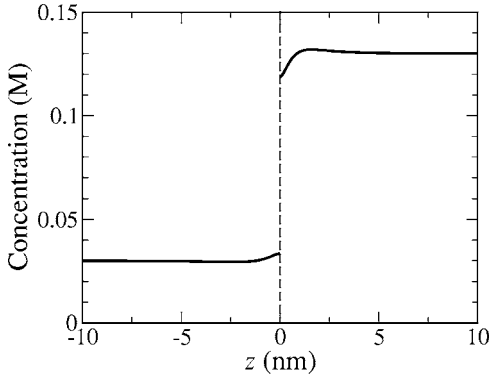

FIG. 6. The density profiles of two neighboring electrolytes versus distance from their interface. The bulk densities are $C_1=0.13M$ and $C_2=0.03M$.

concentrations. As the 1:1 electrolyte shows a modest decrease of C_b/C_0 on C_0, for both 1:2 and 2:2 electrolytes the ratios drop very quickly with C_0. At concentrations larger than those shown in the figure for the 1:2 and 2:2 electrolytes, the density profiles fluctuate in our calculation. This indicates phase separation and criticality which in electrolytes have been studied experimentally [20,21] and theoretically [22]. To treat the phase separation, the DH theory should be extended, such as by considering dipolar pairs in equilibrium with the free ions, adding dipolar ionic solvation free energy, or including hard-core repulsions [22]. For an aqueous 1:1 electrolyte, the critical points are found at temperatures much lower than room temperature [20].

B. Two neighboring electrolyte solutions

Similar depletion behavior also happens when two electrolytes with different average densities are separated by an interface. Consider two electrolyte solutions separated at $z=0$. This could happen for the two electrolytes either (1) having two immiscible solvents or (2) being separated by a thin membrane. In the first case ion transfer across such an interface has been extensively studies in recent years. The structure and potential distribution inside the interface are important factors, and different models have been proposed, along with experimental measurements [23,24]. For the second case the common situations where lipid/surfactant bilayers separating two aqueous regions in either biological or laboratory setups are obvious examples.

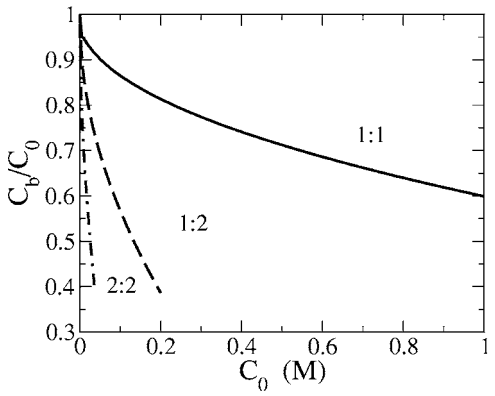

FIG. 5. The ratios between interfacial and bulk electrolyte densities, C_b/C_0, at different C_0 for electrolytes with a water-electrolyte interface. Three curves are shown for the 1:1, 1:2, and 2:2 electrolytes.

The corrections to the mean-field free energy due to the boundary and inhomogeneity can now be used to compute the densities in these two electrolytes. Knowledge of these densities near the boundary is important—e.g., in determining the rate of ion transfer across the immiscible interface or the membrane.

For a test charge located at $z_0\hat{z}$ (assuming $z_0>0$), besides the mean potential contributed from the ions in the electrolyte at $z>0$, the ions at $z<0$ would also contribute a mean potential $\varphi_<$. A similar approximation as used in the first term of Eq. (10) yields

$$\varphi_< \approx \frac{-q\kappa(-z_0)}{4\pi\epsilon}\frac{e^{-2\kappa(-z_0)z_0}}{2},$$

and the total electrostatic free energy per unit area for two electrolytes with the same dielectric constant is obtained as

$$F^{\mathrm{el}} = \frac{1}{12\pi\beta}\int_{-\infty}^{\infty}\left\{-\kappa^3[1-g(\kappa(z)|z|) + g(\kappa(-z)|z|)] + \frac{\kappa^{2\prime\prime}}{8\kappa}\right\}dz. \tag{13}$$

Assume two electrolytes having concentrations C_1 and C_2. Since the ions in one electrolyte are contributing to the electrostatic free energy for ions on the other side of the interface, assuming $C_1>C_2$, we could then expect that $C_1>C_{1b}>C_{2b}>C_2$. For $C_1=0.13M$ and $C_2=0.03M$ the density profiles are shown in Fig. 6, which do show the expected behavior. We are interested in the interfacial concentration difference ΔC_b. The ratio between ΔC_b and the bulk concentration difference ΔC, with $C_2=0.03M$, $0.09M$, and $0.15M$ for the 1:1 electrolyte and $C_2=0.03M$ for the 1:2 electrolyte, are shown in Fig. 7. They are decreasing with increasing of ΔC. The ratio is lower at fixed ΔC with higher C_2 due to the larger electrostatic free energy contribution at higher average

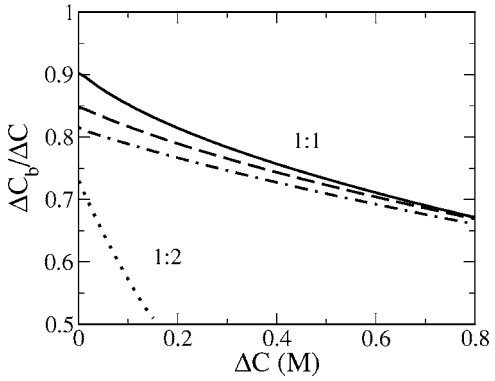

FIG. 7. The ratios between interfacial electrolyte density difference and bulk electrolyte density difference, $\Delta C_b/\Delta C$, at different ΔC. For the 1:1 electrolytes, the solid line is for $C_2=0.03M$, the dashed line for $0.09M$, and the dot-dashed line for $0.15M$. For the 1:2 electrolyte, $C_2=0.03M$.

concentrations. We also see that the decreasing of the ratio on increasing ΔC for the 1:2 electrolyte is very fast.

It is also very interesting to see that at the limit of $\Delta C \to 0$, the ratio $\Delta C_b/\Delta C$ tends to a value depending on C_2. For example, at $C_2=0.03M$ for the 1:2 electrolyte, the interfacial density difference is always less than three-quarters of the bulk values.

C. Attraction between two neutral macrospheres in electrolytes

A pair of charged colloidal spheres in electrolytes are predicted to experience an effective repulsion at large separations by the Derjaguin-Landau-Verwey-Overbeek theory [25]. Recent experiments demonstrated unexpected long-range attractions between like-charged particles under some circumstances. For example, a surprisingly strong attraction was measured in metastable colloidal crystallines [26]. Attractions have been measured for pairs of spheres confined by one or two charged planar walls [27]. Several mechanisms have been proposed, such as the charge fluctuations of colloids and counterions [28], strong counterion correlations [29], nonequilibrium hydrodynamics [30], and the overcharging effect of macroions with excess counterions [31]. Computer simulations show that the imbalanced pressure caused by the depletion zone of counterions between macroions also leads to an effective attraction [32].

In this section we discuss the fact that the depletion of electrolytes around *uncharged* colloids contributes an attraction between two touching colloids. Since the depletion zone width is at the order of the Debye length λ, it is also the effective range of such attraction.

Consider two neutral macrospheres in an 1:1 electrolyte solution. The dielectric constants of the spheres are assumed to be 1. From Fig. 8, two nearly touching spheres would have less total depleted electrolytes than two well-separated ones, with the difference of the depletion zone being approximately the shaded region. For the radius R of the spheres with $R \gg \lambda$, we approximate the electrolyte distribution as that near the flat air-water interface. Recall our results

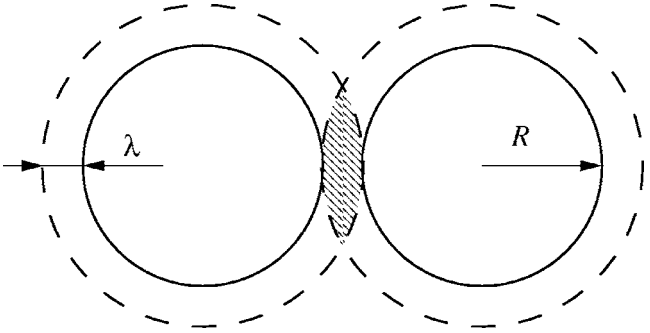

FIG. 8. Two touching macrospheres: The dashed circles represent the depletion zone of electrolytes from the sphere surfaces (solid circles).

in Sec. II where the free energy per unit area needed to create a depletion zone with width at order of λ is obtained as the surface tension σ. As the resulting σ has been shown as the dashed line in Fig. 3, the decreasing of free energy by touching two spheres can quickly be estimated as the product of σ/λ and the volume of the shaded region in Fig. 8, which is calculated to be $\approx 2\pi R\lambda^2$. For concentrations below $0.01M$ the results are shown in Fig. 9.

The free energy difference (dashed line) increases with the electrolyte concentrations. The active range of the interaction is at the order of λ, which is also plotted in Fig. 9. For larger concentrations, the range being very small, additional potentials experienced by the ions—e.g., the dispersion interaction—would be more important than the electrostatic interaction [18]. There are also other interactions between spheres, such as the van der Waal attraction and the interaction between polarized surfaces. The depletion interaction may only contribute a weak attraction at dilute electrolyte concentrations. When λ approaches R, the approximation of an infinite planar interface probably overestimates the depletion.

IV. CONCLUSION

In conclusion we have derived the free energy density of inhomogeneous electrolytes based on the Debye-Hückel

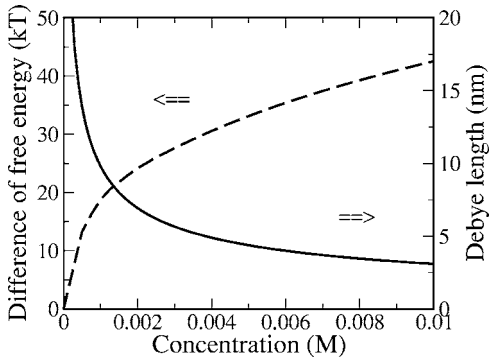

FIG. 9. The free energy difference (dashed curve) caused by the effective depletion zone and the Debye length (solid curve) at different electrolyte concentrations, for two neutral macrospheres with $R=0.3$ μm.

theory. A differential term to the free energy density is obtained under the assumption of a slow-varying electrolyte density. This term would retard the local inhomogeneity. Near the boundary the free energy density is also modified and it is found to repel ions from the boundary. Applying these results to an electrolyte with an air-water interface, the differential and boundary terms dominate the image charge term and cause a larger electrolyte depletion zone nearby the interface than previous theories. Including the consideration of the finite ionic sizes, the predicted surface tension agrees with experimental results at low concentrations. The density profiles of two electrolytes separated by an interface are also considered. The ratio between the interfacial density difference and the bulk difference decreases as the bulk difference increases. This would be important to the question of ion transfer across the interface. Finally, we show that the electrolyte depletion produces an attraction ($\sim 18\ k_BT$ at electrolyte concentrations $\sim 0.001M$ for macroions with 0.3 μm radii) in typical experiment conditions between two neutral spheres when their separation is at the order of the Debye length.

ACKNOWLEDGMENT

The support of National Science Council of Taiwan is acknowledged.

[1] P. W. Debye and E. Hückel, Phys. Z. **24**, 185 (1923).
[2] D. A. McQuarrie, *Statistical Mechanics* (Harper & Row, New York, 1976).
[3] C. Wagner, Phys. Z. **25**, 474 (1924).
[4] N. Bjerrum, K. Dan. Vidensk. Selsk. Mat. Fys. Medd. **7**, 1 (1926).
[5] L. Belloni, Phys. Rev. Lett. **57**, 2026 (1986); J.-P. Hansen and I. McDonald, *Theory of Simple Liquids* (Academic, London, 1990); R. D. Groot, J. Chem. Phys. **94**, 5083 (1991); M. Lozada-Cassou and J. E. S. Sanchez, Chem. Phys. Lett. **190**, 202 (1992).
[6] See, e.g., J. P. Valleau, J. Chem. Phys. **95**, 584 (1991); P. Linse and V. Lobaskin, Phys. Rev. Lett. **83**, 4208 (1999); J. Reščič and P. Linse, J. Chem. Phys. **114**, 10131 (2001).
[7] S. Nordholm, Chem. Phys. Lett. **105**, 302 (1984).
[8] M. N. Tamashiro, Y. Levin, and M. C. Barbosa, Physica A **268**, 24 (1999).
[9] L. Mier-y-Teran, S. H. Suh, H. S. White, and H. T. Davis, J. Chem. Phys. **92**, 5087 (1990); Z. Tang, L. E. Scriven, and H. T. Davis, *ibid.* **97**, 494 (1992); T. Biben, J.-P. Hansen, and Y. Rosenfeld, Phys. Rev. E **57**, R3727 (1998); D. Boda, D. Henderson, R. Rowley, and S. Sokolowski, J. Chem. Phys. **111**, 9382 (1999).
[10] J.-L. Barrat and J.-P. Hansen, *Basic Concepts for Simple and Complex Liquids* (Cambridge University Press, London, 2003).
[11] M. C. Barbosa, M. Deserno, and C. Holm, Europhys. Lett. **52**, 80 (2000); M. C. Barbosa, M. Deserno, C. Holm, and R. Messina, Phys. Rev. E **69**, 051401 (2004).
[12] L. Onsager and N. N. T. Samaras, J. Chem. Phys. **2**, 528 (1934).
[13] A. Heydweiller, Phys. Z. **3**, 329 (1902).
[14] D. Myers, *Surface, Interfaces, and Colloids: Principles and Applications* (VCH, New York, 1991).
[15] Y. Levin, J. Chem. Phys. **113**, 9722 (2000); Y. Levin and J. E. Flores-Mena, Europhys. Lett. **56**, 187 (2001).
[16] The restriction of integration domain to $z>0$ in Eq. (6) also leads to a contribution to Eq. (9). However, its magnitude is much smaller than Eq. (9) and changes very little of the latter numerical results.
[17] N. Matubayasi, H. Matsuo, K. Yamamoto, S. Yamaguchi, and A. Matuzawa, J. Colloid Interface Sci. **209**, 398 (1998).
[18] B. W. Ninham, and V. Yaminsky, Langmuir **13**, 2097 (1997); M. Boström, D. R. M. Williams, and B. W. Ninham, *ibid.* **17**, 4475 (2001).
[19] C.-H. Ho, H.-K. Tsao, and Y.-J. Sheng, J. Chem. Phys. **119**, 2369 (2003).
[20] H. Glasbrenner and H. Weingärtner, J. Phys. Chem. **93**, 3378 (1989).
[21] R. R. Singh and K. S. Pitzer, J. Chem. Phys. **92**, 6775 (1990); T. Narayanan and K. S. Pitzer, Phys. Rev. Lett. **73**, 3002 (1994); M. A. Anisimov, A. A. Povodyrev, V. D. Kulikov, and J. V. Sengers, *ibid.* **75**, 3146 (1995).
[22] M. E. Fisher and Y. Levin, Phys. Rev. Lett. **71**, 3826 (1993); Y. Levin and M. E. Fisher, Physica A **225**, 164 (1996).
[23] E. J. W. Verwey and K. F. Niessen, Philos. Mag. **28**, 435 (1939); H. H. Girault and D. J. Schiffrin, J. Electroanal. Chem. Interfacial Electrochem. **150**, 43 (1983).
[24] T. Wandlowski, V. Marecek, K. Holub, and Z. Samec, J. Phys. Chem. **93**, 8204 (1989); T. Kakiuchi, J. Noguchi, M. Kotani, and M. Senda, J. Electroanal. Chem. Interfacial Electrochem. **296**, 517 (1990); T. Kakiuchi, J. Noguchi, and M. Senda, *ibid.* **336**, 137 (1992).
[25] B. V. Derjaguin and L. D. Landau, Acta Physicochim. URSS **14**, 633 (1941); E. J. W. Verwey and J. T. G. Overbeek, *Theory of the Stability of Lyophobic Colloids* (Elsevier, Amsterdam, 1948).
[26] A. E. Larsen and D. G. Grier, Nature (London) **385**, 230 (1997).
[27] G. M. Kepler and S. Fraden, Phys. Rev. Lett. **73**, 356 (1994); J. C. Crocker and D. G. Grier, *ibid.* **77**, 1897 (1996); D. G. Grier, Nature (London) **393**, 621 (1998).
[28] O. Spalla and L. Belloni, Phys. Rev. Lett. **74**, 2515 (1995); B.-Y. Ha and A. J. Liu, *ibid.* **79**, 1289 (1997).
[29] N. Grønbech-Jensen, R. J. Mashl, R. F. Bruinsma, and W. M. Gelbart, Phys. Rev. Lett. **78**, 2477 (1997).
[30] T. M. Squires and M. P. Brenner, Phys. Rev. Lett. **85**, 4976 (2000).
[31] R. Messina, C. Holm, and K. Kremer, Phys. Rev. Lett. **85**, 872 (2000).
[32] E. Allahyarov, I. D'Amico, and H. Löwen, Phys. Rev. Lett. **81**, 1334 (1998).